Optimization of sensor based on surface plasmon resonance for indicating harmful substances in the air

Anna M. Ivanchenko[1, 2], Ildus S. Khasanov[2]
[1] Bauman Moscow State Technical University
[2] STC UI RAS
[1, 2] Moscow, Russian Federation
[1] ivanchenko.anna.m@gmail.com, [2] khasanov@ntcup.ru

Anna M. Ivanchenko[1, 2], Ildus S. Khasanov[2]
[1] Bauman Moscow State Technical University
[2] STC UI RAS
[1, 2] Moscow, Russian Federation
[1] ivanchenko.anna.m@gmail.com, [2] khasanov@ntcup.ru

Abstract: **Surface plasmon resonance (SPR) sensors have various applications, one of which is to indicate harmful substances in the air. In this paper, we optimize the sensitivity of the SPR sensor with the adaptive Monte-Carlo method to use it in terms of the detection of toxins, in particular chlorine, in the air. We find the optimal parameters in the Kretschmann configuration, which is suitable for the detection of silver chloride with the red LEDs, resonance angle between 40 and 80 degrees, and the thickness of the silver film between 40 and 80 nm in the scheme.**

Keywords– sensor, SPR, toxins, optimization, adaptive.

I. Introduction

Air pollution has a serious impact on human health. WHO estimates that air pollution causes millions of premature deaths worldwide every year. Scientific evidence suggests that indoor air pollution may be higher than outdoor air pollution in large and industrialized cities [1]. Of these, 90 percent are from low- or middle-income countries. In children, air pollution can cause impaired development and lung functions, respiratory infections, and aggravation of asthma. Among the most common causes of death caused by air pollution in adults, ischaemic heart disease and stroke are mentioned.

Let's compare the maximum permissible concentration and the threshold of smell perception: for Chlorine, the maximum one-time MPC is 0.1 mg/m^3, while the threshold for smell perception is 2-3 mg/m^3. In the case of sulfur dioxide, the maximum one-time MPC is 0.5 mg/m^3 and the odor perception threshold is 21 mg/m^3. From this data, we can make a conclusion, that for some substances the odor perception threshold may be significantly higher than the MPC. This means that toxic gases can have a latent adverse effect on human health. Therefore, it is important to detect such effects using devices without relying on sensory organs.

Nowadays for detecting air pollution thresholds use gas analyzers – instruments for determining the qualitative or quantitative composition of gas mixtures. The most common are portable chemical gas analyzers. The working principle is based on the measurement of the reduction of the sample of combustion products as a result of the absorption of individual gas components by chemical reagents. The disadvantage of this type of instrument is its short-term operation, which requires the permanent replacement of the chemical agent, making it difficult to use it for continuous measurements. The principle of optical gas analyzers is based on the measurement of the optical properties of the analyzed gas mixture, such as spectral absorption, optical density, refractive index, and spectral radiation. Usually, their measurement principle is based on the selective absorption of gases and vapors in infrared radiation. Despite the high sensitivity, and the possibility of continuous measurements, drawbacks are the attraction of complex spectral technology, which can significantly increase the ultimate cost of the device. Thus, the devices sensitive to low concentrations of toxic substances in the air are expensive. This means that high costs create barriers to their widespread use.

Alternative for detecting the influence of small concentrations of poisonous substances on the human body is the development of accumulative sensors, that analyze the composition of the air over a long period of time and provide information on the effects of harmful substances on the human body in a day, day or week. One possible way to develop it is to use surface plasmon resonance (SPR).

The method is based on the corrosion effect of silver film in the presence of toxic substances in the air. Moisture in the crust is a good solvent and, when interacting with toxic substances, can form weak solutions of acids, condensation of which leads to corrosion of metal surfaces and corrosion film. The rate and nature of its appearance can be tracked by the Python-based surface plasmon resonance method, drawing conclusions about the presence of toxic substances in the air.

The developed indicator based on the SPR combines the principles of optical and chemical gas analyzers. Due to the high sensitivity of plasmonic methods, the relative durability, and the cheapness of dusting thin metal films, this sensor has good prospects for development.

The result of the study will be a developed indicator based on surface plasmon resonance for detecting the accumulated influence of harmful substances in the air on the human body. The device will act as an «indicator of healthy air» in places where people congregate: in gardens and schools, in offices, and at enterprises. It will collect information on the state of air in passive mode and warn of exceeding the average daily MPC, which will save people from the influence of low concentrations of toxic substances by eliminating the cause of pollution in a timely manner.

The scientific novelty consists in the optimization of the sensitivity of the sensor by using the Monte-Carlo method combined with the algorithm of construction of resonance curves, which take into account the diverse nature of corrosion changes on the silver surface depending on the input parameters.

This work includes a study on the use of plasmon resonance techniques for the analysis of toxic air content. Its main goal was to optimize the sensitivity of the method for the detection of harmful substances in air based on SPR by correcting the parameters involved in the indicator model.

979-8-3503-9952-3/23/$31.00 ©2023 IEEE

This study could provide the basis for the development of an instrument to assess the average daily concentration of harmful substances in the air. The indicator will be able to report whether there are toxic substances in the air above the average daily MPC, i.e. in sufficient quantities to cause long-term harm to humans. The device is designed to detect small concentrations of toxic substances in the air and their accumulated effects on the human body.

II. THE PLASMON RESONANCE

Surface plasmon polaritons (SPP) arise from the interaction of electromagnetic dielectric fields with electron plasmon. They are surface excitations spreading in a sufficiently thin layer along the boundary between the conductor and the dielectric.

We note that SPP has a borderline frequency of existence. This is due to the fact that superficial excitations exist only as long as volume excitation is difficult. The boundary frequency between the excitation of surface and volumetric waves for plasmons is its own frequency of electron gas of metal (plasmon frequency $\omega_p/\sqrt{2}$). At frequencies lower than this, only SPP is possible. In addition, the wave vector of the SPP propagating along the metal surface differs from the wave vector of the volumetric plasmon. The relationship between the SPP k_x wave vector and the frequency ω (quantum energy) of the SPP is described by the dispersion relation of the form:

$$k_x = \frac{\omega}{c}\sqrt{\frac{\varepsilon_d\,\varepsilon_m}{\varepsilon_d+\varepsilon_m}} \tag{1}$$

where c is the speed of light, ε_d and ε_m are the complex dielectric permeability of the dielectric and metal layer.

It follows from the formula that each frequency of light corresponds to its own wave vector to excite the SPP. This method of excitation is called resonant, since in the case of illumination of the surface by a non-monochromatic beam of light, only light quanta for which the laws of energy conservation and impulse are fulfilled will excite the SPP.

To fulfill the terms of the alignment of wave vectors, there are various schemes of light input.

Consider prism input – i.e. the transformation of light into surface electromagnetic waves (SEW) by a prismatic method. It is based on the phenomenon of broken full internal reflection at the fall of p-polarized radiation, on the surface-active medium from the optically denser medium. The prism input exists in two configurations: Otto geometry and Kretschmann geometry.

Our study used the Kretschmann geometry, which is widespread in the plasmon range (Fig. 1). A thin metal film is sprayed onto a glass prism. Photons that are reflected from the boundary between the prism with dielectric permeability ε and metal will have enough momentum to trigger the SPP at the boundary between metal and air. This method excites SEW on a smooth surface because the transformation of the volumetric radiation into SEW allows the alignment of their wave vectors. The SPP is triggered by a change in the intensity of the reflected beam.

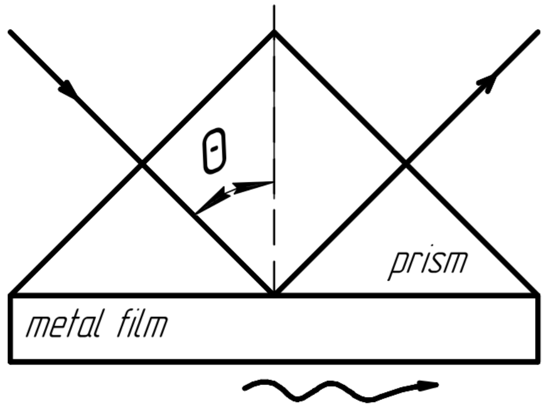

Fig. 1. Plasmon injection method for SPP excitation using broken full internal reflection in Kretschmann configuration.

In the case of frustrated total internal reflection, the plasmon resonance phenomenon analysis is based on the determination of the reflectance coefficient of R of the incident light at an angle greater than the angle of full internal reflection in the prism. The reflectance coefficient R is reduced when the excited SPP takes part of the energy of the incident light. The illustrative graph of the ratio of reflection to the angle θ is given in Fig. 2 and is described by the approximate equation:

$$R(\theta) = 1 - \frac{\alpha^2}{(\theta - \theta_r)^2 + a^2} \tag{2}$$

where θ_r is the resonance angle, α is the excitation coefficient of the SPP, a is the half-width of the resonance curve.

Fig. 2 shows that the SPP is not triggered by a specific angle of fall, but by a set of angles. This set of angles corresponds to a set of photon pulses (a set of wave vectors). The reason for this lies in the final lifetime of the PP. The large width of the resonance curve corresponds to a large dispersion in PP energy, that is, their short lifetime. And the longer the lifetime of the plasmon, the stronger the interaction, the more energy is converted to the SPP, and thus the greater the sensitivity of the method to changes in the metal film.

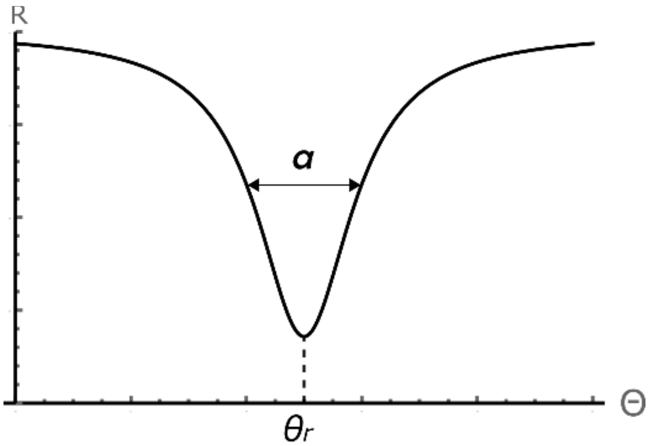

Fig. 2. Example of a resonance curve R(θ). R is reflectivity, θ is the angle (˚).

III. THE MODEL OF THE SENSOR

A. Operation bases

The principle of operation of the proposed indicator of harmful substances is based on the effect of corrosion of

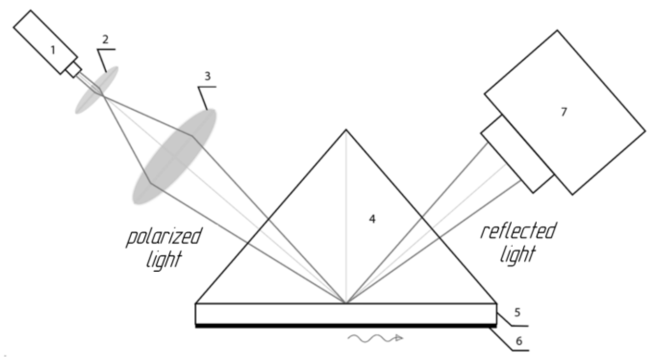

Fig. 3. The scheme of the indicator of small concentrations of harmful substances is based on surface plasmon resonance.

metals when interacting with chemically active substances. The Earth’s atmosphere is always moist and water is a good solvent. Harmful substances, such as chlorine, form weak solutions of acids such as hydrochloric acid when interacting with water. Moisture from the air is continuously deposited by a thin layer on surfaces, including metal surfaces. After condensation, small drops of water-reactive solutions of acids begin to interact with the metal, forming a corrosive film on the surface. We can track the changes in air composition by regularly scanning the changing corrosive layer on the surface of the thin metal film.

The beam of light passes through the lens system and the polarizer focuses at the center of the hypotenuse prism at a resonance angle and causes a surface plasmon resonance on the surface of a thin silver metal film. The reflected beam falls on the camera, where it is read and analyzed using the numpy and matplotlib libraries in python. Over time, a corrosive layer is formed on the surface of the metal film. At the same time, the type of the resonance curve, its depth, width, and extrema vary depending on the composition and speed of the appearance of the corrosive film. Comparing graphs in the initial period of time with those obtained after a period of time will allow drawing conclusions about the presence or absence in the air of harmful substances dangerous to humans.

The scheme of the sensor based on this principle is shown in Fig. 3. It includes:

1 – laser

2, 3 – lens system with polarizer

4 – glass prism

5 – thin metal film (Ag)

6 – corrosion layer (AgCl)

7 – camera

B. Configuration before corrosion started

Let's take a look at the initial position of our sensor. There are only 3 layers in this scheme (Fig. 4) because the corrosion process has not yet started. The first layer is a glass prism with the relative permittivity ε_1, the second is a thin silver metal film (Ag) with the ε_2, and the last one is air with the relative permittivity $\varepsilon_3 = 1$.

The function for reflectivity, in this case, is described by the (3).

$$R^t = \left|\frac{r_1^2 + r_2^3 \exp(2idw_2)}{1 + r_1^2 r_3^3 \exp(2idw_2)}\right|^2 \cdot \left|1 - \left(r_0^1\right)^2\right|^2 \qquad (3)$$

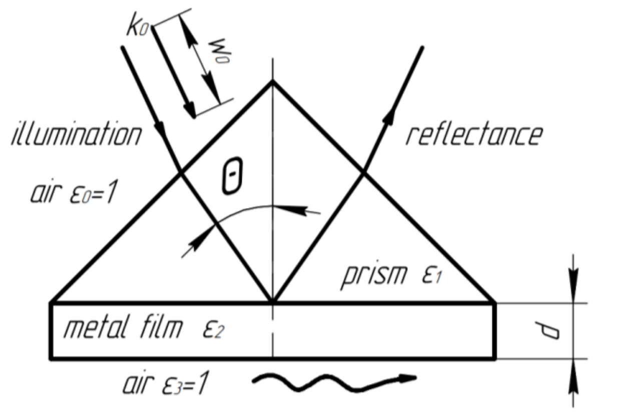

Fig. 4. Experimental setup used at the beginning of air analyses

where, R – reflectivity, r_{ij} – amplitude reflection coefficients for p-polarization, d – thickness of a metal layer on the prism, w_2 – normal to wave vector, which can be calculated by (4).

$$w_i = \frac{2\pi\sqrt{\varepsilon_i - \varepsilon_1 \sin^2\left(\varphi_g\right)}}{\lambda_0} \qquad (4)$$

where ε_1 is the relative permittivity of the glass prism, ε_i is the relative permittivity of other layers in the scheme (i = 2, 3…) and λ_0 is an illumination wavelength.

C. Configuration after corrosion started.

If there are harmful substances in the air, a corrosive layer will gradually appear on the surface of the silver metal film sometime after the start of the indicator operation. In this case, there will be 4 layers in the reflectivity function (5), and the scheme can be described in Fig. 5. The first layer is a glass prism with the relative permittivity ε_1, the second is a thin silver metal film (Ag) with the ε_2, the third one is a corrosion layer with the relative permittivity ε_3 and the last is air with the relative permittivity $\varepsilon_4 = 1$.

To simulate and optimize the resonance curve in a scheme with an additional dielectric layer (corrosion layer), we can refer to the following function:

$$R = \left|\frac{r_1^2 + r_2^3 e^{2id_2w_2} + r_3^4 e^{2i(d_2w_2+d_3w_3)} + r_1^2 r_3^3 r_3^4 e^{2id_3w_3}}{1 + r_1^2 r_3^3 e^{2id_2w_2} + r_1^2 r_3^3 e^{2i(d_2w_2+d_3w_3)} + r_3^3 r_3^4 e^{2id_3w_3}}\right|^2 \left|1 - (r_0^1)^2\right|^2 \qquad (5)$$

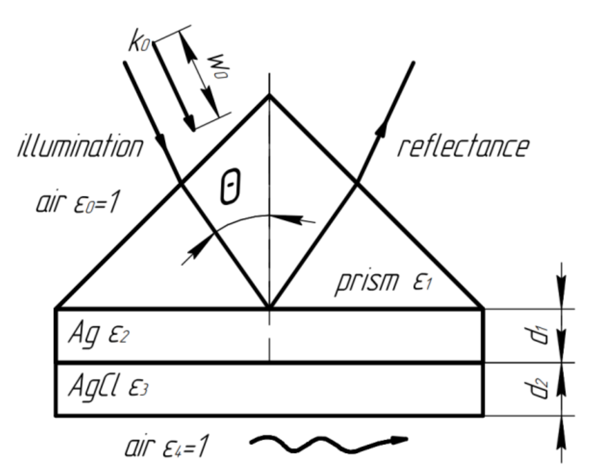

Fig. 5. Experimental setup after metal corrosion started.

where, R – reflectivity, r_{ij} – amplitude reflection coefficients for p-polarization, d – thickness of the thin silver film, w_2 – normal to wave vector, (4).

The coefficients r_i^{i+1} depend on the polarization and on the permittivities of two successive media.

1) in (s) polarization:

$$r_i^{i+1} = \frac{w_i - w_{i+1}}{w_i + w_{i+1}} \quad (6)$$

2) in (p) polarization:

$$r_i^{i+1} = \frac{\varepsilon_{i+1} w_i - \varepsilon_i w_{i+1}}{\varepsilon_{i+1} w_i + \varepsilon_i w_{i+1}} \quad (7)$$

IV. THE OPTIMIZATION OF THE SENSITIVITY OF THE SENSOR

A. *Sensitivity of the Model*

The sensitivity of the sensor determines the quality of analysis of harmful substances in the air and the accuracy of data. It is the most important characteristic of any sensor. That is why to use the SPR method, optimization is necessary. Basically, the sensitivity depends on the following parameters: the thickness of the metal film d_1, the refractive index of prism n_0, the wavelength λ, and the resonance angle θ. We can consider the combination of parameters of the indicator optimal when it leads to the value of the reflectance coefficient R close to zero [3]. To detect specific gases in the air, such as chlorine, it is important to ensure a high sensitivity for this particular dielectric. For this reason, we add the corrosion layer thickness of d_2 and its dielectric permeability eps_2 to the list of parameters for optimization.

B. *Optimization method*

The optimization target is the smallest value of the R because this condition prevents the main task of optimization – high sensitivity. The Monte-Carlo method, as a well-known tool for studying the model's sensitivity, was chosen to find a combination of parameters satisfying this optimization criterion. This optimization strategy involves the random generation of endogenous parameters and the statistical analysis of model results, but in this case, we use adaptive boundaries in order to improve the efficiency of the method. This means the following: after the generation of the number N families p of random parameters in the set boundaries of search [Bmin, Bmax], we select combinations of parameters ps suitable for the condition $R(p) \in [0, 10^{-2}]$ and update the p boundaries to the ps boundaries, after which starts a new iteration with the boundaries contains the successful results of the previous loop. This adaptive method enables us to increase the length of ps after each iteration, which helps us to get results quickly. The course description of this adaptive Monte-Carlo method is given in Algorithm 1.

To detect harmful substances in the air, such as chlorine, we set the physically acceptable interval for the parameters and a tolerance of R between 0 and 10^{-2}. We also optimize the sensor response to determine the relative permittivity of silver chloride (AgCl) ε_3 [1.9004; 2.0668], wavelength λ limited by the area of red LEDs [600; 700] nm, the refractive index of the prism is $n_1 \in [1.4; 1.8]$, the resonance angle $\theta \in [40^\circ; 80^\circ]$, and the thickness of the silver film $d_1 \in [40; 60]$ nm. The relative permittivity of the silver ε_2 is given by the Drude model (8).

$$\varepsilon_2 = 1 - \frac{\omega_p^2}{(1/\lambda)^2 + i\cdot\gamma\cdot(1/\lambda)} \quad (8)$$

where $1/\lambda = \omega_l$ is angular frequency of light in rad/s, the $\omega_p \in [69370; 77430]$ and $\gamma \in [145.2; 363]$.

Therefore, the input vectors are as follows: Bmin = {40, 40, 600, 1.9004, 1.4, 69370, 145.2}, Bmax = {60, 80, 700, 2.0668, 1.8, 77430, 363.0}. With N = 20.000, the thickness of the silver chloride d_2 = 1 nm, and tolerance on R $\alpha = 10^{-2}$, more than 8000 iterations are required in the loop to optimize all the set boundaries. The input data and the results of the optimization are summarized in Tab.1.

C. *Algorithm 1. Code for the adaptive Monte-Carlo algorithm.*

Input: α (tolerance on R), N (the number of random parameters set at each iteration), d_2 (the thickness of the silver chloride layer). The initial boundaries of the matrix of acceptable parameters are set: Bmin = {min(d_1), min(θ), min(λ), min(ε_3), min(n_0), min(ω_p), min(γ)} and Bmax = {max(d_1), max(θ), max(λ), max(ε_3), max(n_0), max(ω_p), max(γ)}.

The loop:

1) Generate random parameters set p in the input boundaries Bmin, Bmax.

2) Calculate the value of the reflectivity R({p}) for each generated combination of elements in the matrix p and create a new matrix y with all the values

3) Select the vectors in {y} that verify the condition of optimization R < α and create a new matrix ps with the selected vectors.

4) Update the initial boundaries to the boundary values of new matrix elements ps: Bmin = min{ps}, Bmax = max{ps}.

5) Generate random parameters set p in the boundaries Bmin, Bmax.

6) Calculate the value of the reflectivity R({p}) for each generated combination of elements in the matrix p and create a new matrix y with all the values

7) Select the vectors in {y} that verify the condition of optimization R < α and create a new matrix ps with the selected vectors.

8) As long as the length of ps < N repeat the iteration from the beginning, with the updated

9) When length({ps}) ≥ N end.

TABLE I. INPUT PARAMETERS OF THE MODEL IN THE PHYSICALLY ACCEPTABLE INTERVAL. THE OUTPUT INTERVALS CORRESPOND TO $R < 10^{-2}$.

Parameter	Input interval	Output interval
d_1 (nm)	[40, 60]	[50.9765, 69.2085]
θ (˚)	[40, 80]	[40.5923, 41.6982]
λ (nm)	[600, 700]	[653.0408, 682.3613]
ε_3	[1.9004, 2.0668]	[1.9453, 2.0207]
n_1	[1.4, 1.8]	[1.4171, 1.4493]
ω_p	[69370; 77430]	[71564, 75243]
γ	[145.2; 363.0]	[204.20, 303.78]

The results of optimization are the set of intervals, corresponding to the optimization target R < 10^{-2}. The thickness of the relative permittivity of silver chloride after optimization became ε_3 [1.9453, 2.0207], wavelength λ now limited by the interval [653.0408, 682.3613] nm, the refractive index of the prism changed to $n_1 \in [1.4171, 1.4493]$, the resonance angle $\theta \in [40.5923, 41.6982]$, and the thickness of the silver film $d_1 \in [50.9765, 69.2085]$ nm. The relative permittivity of the silver ε_2, which was given by the Drude model, is also updated: $\omega_p \in [71564, 75243]$ and $\gamma \in [204.20, 303.78]$.

V. Conclusion

In this work, the optimization of the sensor of harmful substances in the air was carried out to enhance the sensitivity of the device. Digital optimization of sensors is necessary also for both time and money. We used adaptive boundaries in the Monte-Carlo optimization method to provide the higherst sensitivity possible. But, in the case of plasmonic sensors, precise sensor modeling remains a challenge. The optimization methods themselves must be thoroughly tested before they can be applied to plasmonics. However, these results can be used to develop a new type of gas analyzer – an indicator of the harmful substances in air based on surface plasmon resonance.

Acknowledgment

We thank lobastov S. A. for providing glass prism with thin metal film, Batshev V. I. (BMSTU), Blagova T. V. (BMSTU), and Nikitin P. A. (STC UI RAS) for assistance in digital modeling and for comments on the paper. This work was supported by the Bauman Moscow State Technical University.

References

[1] Leygraf C. et. all. Atmospheric corrosion // Hoboken, New Jersey: Wiley, 2016. 374 p.

[2] Hasanov I.S., Ivanchenko A.M. Development of an indicator of the accumulated effect of small concentrations of harmful substances in air based on surface plasmon resonance // Methods and means of scientific research: Mat. Ph. .D. 2: STC UPU RAS, 2021. P. 8-12.

[3] Barchiesi D. Numerical Optimization of Plasmonic Biosensors // 2011

[4] Barchiesi D. Numerical retrieval of thin aluminium layer properties from SPR experimental data // 2012

[5] Mayer S. A. Plasmonics // Theory and Applications. Regular and chaotic dynamics, 2011. 278 p.

[6] Klimov V. V. Nanoplasmonika // Moscow: Physizmatlite, 2010. Ex. 2. 480 p.

[7] Knyazev B. A. Surface Electromagnetic Waves: from the visible range to the microwave // Bulletin of the Novosibirsk State University. Series: Physics. 2007. T. 2. 1. P. 108-122.

[8] Pavlenko V. A. Gas analyzers // M.-L., 1965.